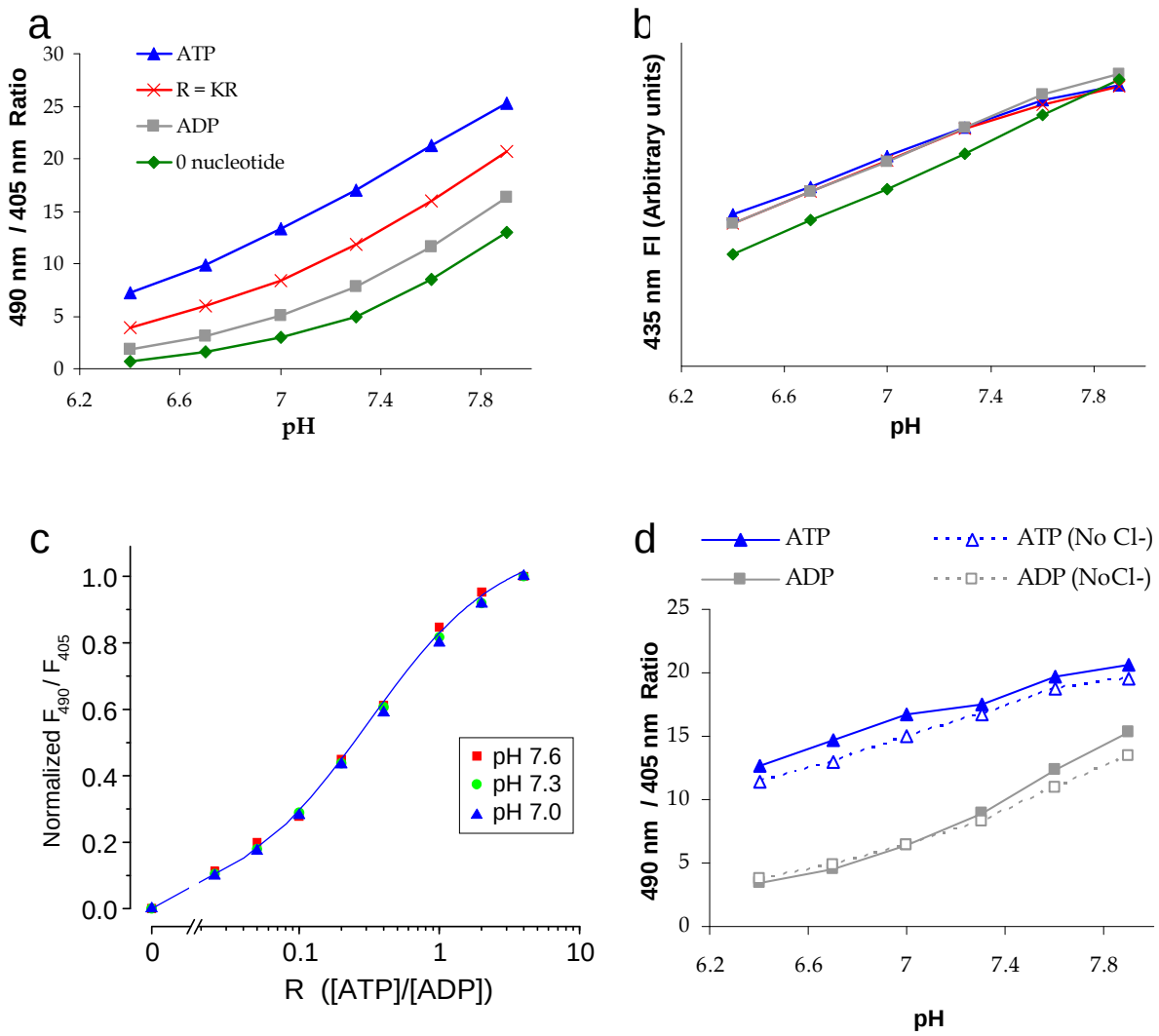

Supplementary Figure 1 | pH and chloride sensitivity of the QV5 construct. (**a,b**) pH titrations of purified QV5 construct when maximally activated (*blue*), half maximal (*red*), ADP (*gray*), and nucleotide free (*green*) solutions. The 490 / 405 Ratio signal (**a**) exhibits a pH sensitivity that is somewhat parallel between the four signals, indicating that pH is not affecting the ATP response, but is clearly affecting the underlying fluorescence of the sensor. The 435 nm signal (**b**) is isosbestic with respect to ATP / ADP ratio across pH values. (**c**) The dose-response to ATP is relatively unaffected by changes in pH. (**d**) Across a range of pH values, the presence (100 mM KCl) or absence (0 KCl) of chloride does not lead to a substantial change in the QV5 construct ratio.

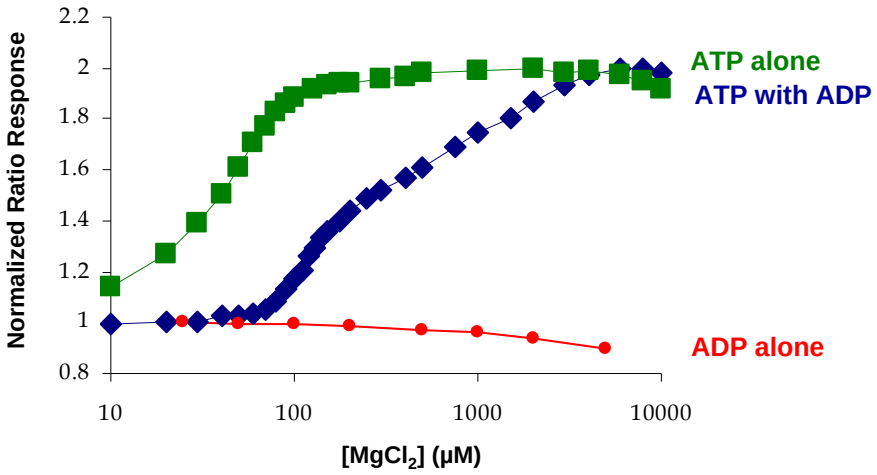

Supplementary Figure 2 | Magnesium Sensitivity of the QV5 construct. The magnesium sensitivity of purified QV5 construct assayed by starting in a magnesium-free solution (with 50 µM EDTA to chelate any contaminating magnesium), then adding $MgCl_2$ to a solution that contains ATP alone (sodium salt, 10 µM, green symbols), ADP alone (potassium salt, 10 µM, red symbols), or a mixture of ATP and ADP (10 µM and 50 µM respectively, blue symbols). As ATP alone binds magnesium (green), the ratio response (490 nm / 405 nm) increases to a maximal value, indicating the requirement of magnesium for the ATP response. As magnesium binds ADP (red), the signal does not increase, indicating magnesium in the binding site, when bound to ADP, does not lead to a maximal fluorescence response. As magnesium is added to the ATP and ADP mixture (blue), low levels of magnesium lead to a half maximal response (as magnesium binds to ATP); we conclude that higher magnesium levels chelate ADP, which then leaves the binding site resulting in a maximal fluorescence response.

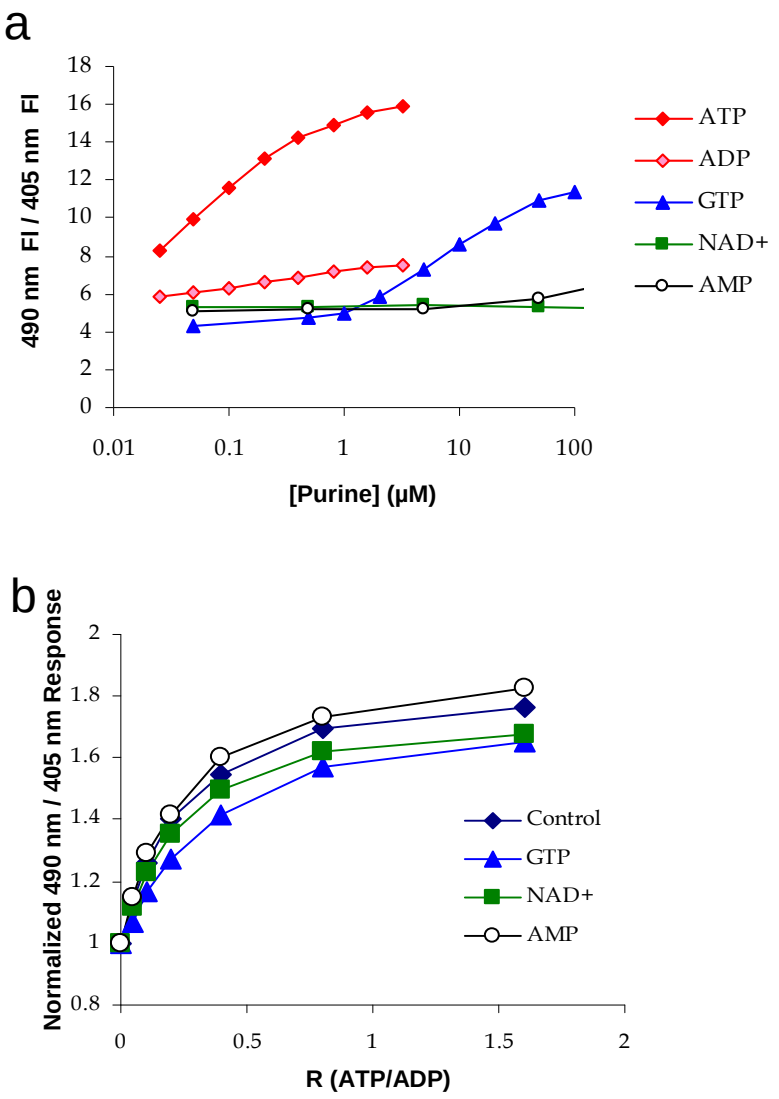

Supplementary Figure 3 | Sensitivity of the QV5 construct to other purine nucleotides. (**a**) Application of NAD^+ or AMP alone gave no increase in the signal from purified QV5 construct. Application of GTP shows a sub-maximal increase with an affinity of ~10 µM, indicating the response is 250 times more selective for ATP than for GTP. (**b**) The ATP / ADP ratio response is unaffected by the constant presence of 1 mM NAD^+ or AMP (with [ADP] = 0.5 mM). Competition with 1 mM GTP may cause a slight reduction in the ATP / ADP affinity.

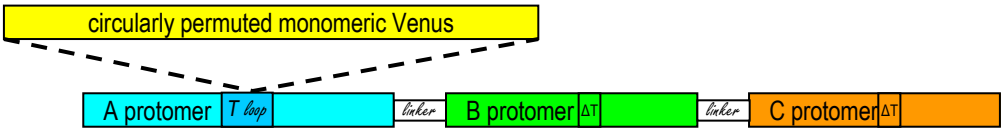

cpmVenus insertion: *RYRGREY*$_{51}$ **– SAG –** *YNSD … KLEYN* **– GT –** *I*$_{52}$*VD*

A-B linker: *TKEEG*$_{108}$ **– ASGGGSGGGGASG –** *M*$_1$*KKVE*

ΔT loop (B & C protomers): *SEVKGR*$_{36}$ **– GAGGG –** *D*$_{54}$*LIPK*

B-C linker: *TKEEG*$_{108}$ **– ASGGGGGSGGASG –** *M*$_1$*KKVE*

Supplementary Figure 4 | Construction of a tandem trimer version of the sensor. A single gene was constructed, encoding a tandem trimeric GlnK1 with a circularly permuted monomeric Venus inserted only in the first protomer. The first protomer is full length, with cpmVenus inserted between positions 51 and 52. In the sequence diagram, numbered subscripts indicate positions in monomeric wildtype GlnK1; black residues indicate linker sequences. The second and third protomers (labeled B and C) have a deletion of the T-loop region, as shown. When expressed in bacteria, the sensor has an N-terminal his-tag (sequence is MKHHHHHHHGAS) preceding the normal N-terminal methionine). The full-length sensor, without the his-tag, is 579 amino acids in length.

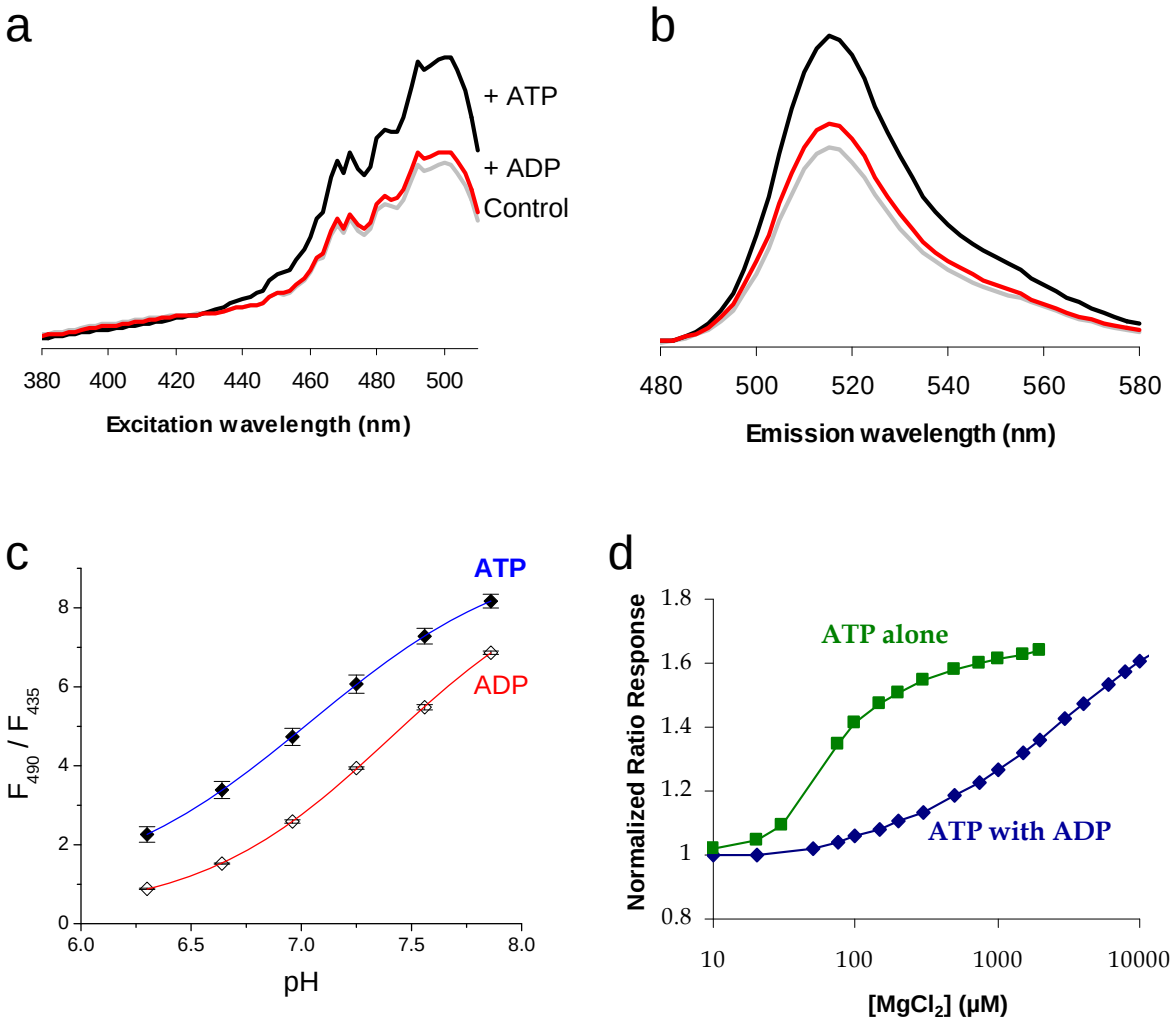

Supplementary Figure 5 | Spectral properties of Perceval. (**a**) Excitation spectra of purified Perceval during control conditions (gray) and following addition of 10 µM ADP (red) or 50 µM MgATP (black), emission at 530 nm. ATP addition leads to an increase in the 490 nm peak and a decrease in the 405 nm peak. (**b**) The shape of the emission spectra, from control (gray) to ADP bound (red) or ATP-bound (black) does not change, excitation wavelength 460 nm. (**c**) Perceval exhibits similar pH sensitivity (compare with **Suppl. Fig. 1**) to the original QV5 construct. Blue and red lines represent fits to data that are used for cellular pH calibration (**Fig. 5**). (**d**) Magnesium sensitivity of Perceval (compare with **Suppl. Fig. 2**) is also comparable to the original QV5 construct. $MgCl_2$ was added to a solution that contains ATP alone (sodium salt, 10 µM, Green symbols) or a mixture of ATP and ADP (10 µM and 50 µM respectively, Blue symbols).

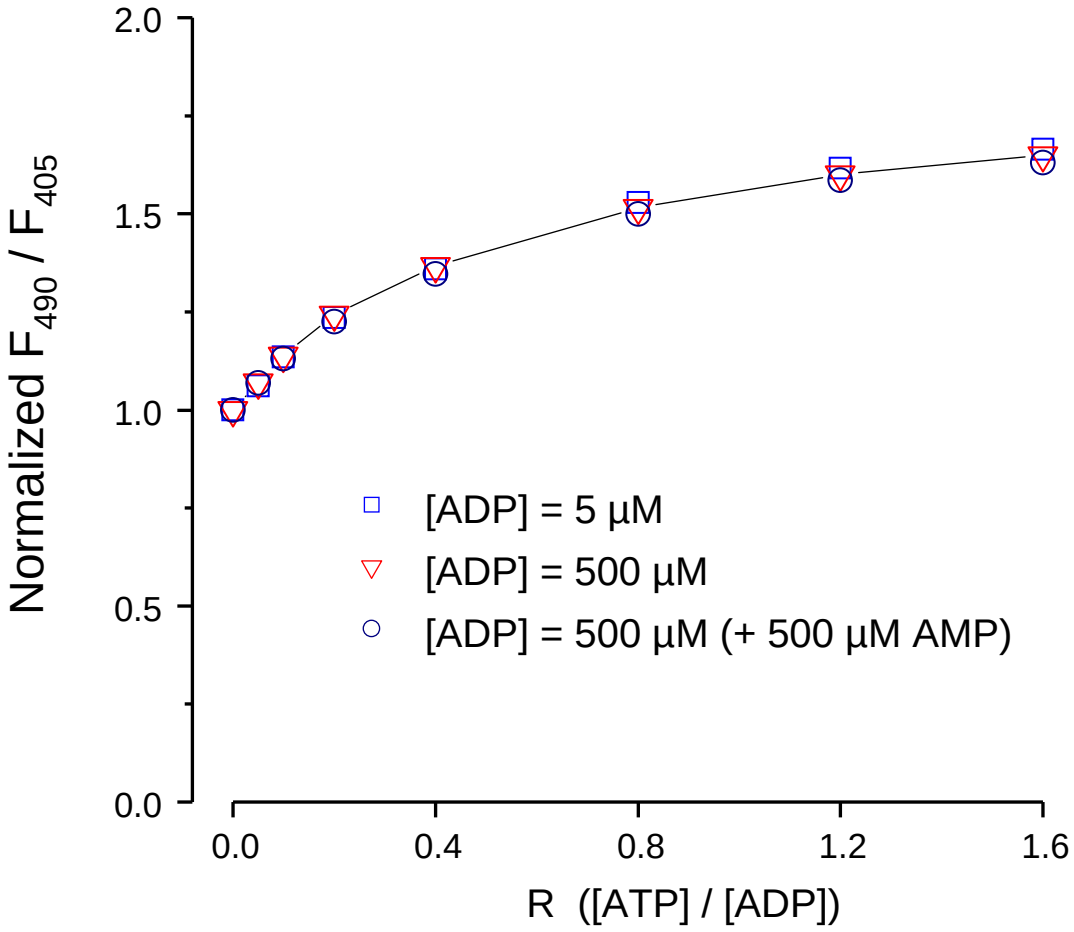

Supplementary Figure 6 | Response properties of Perceval. As seen for QV5 in **Figure 2** of the main paper, Perceval responds to the ATP/ADP ratio over a wide range of absolute concentration (shown here for [ADP] = 5 µM and 500 µM). The presence of 500 µM AMP has no effect on the response.

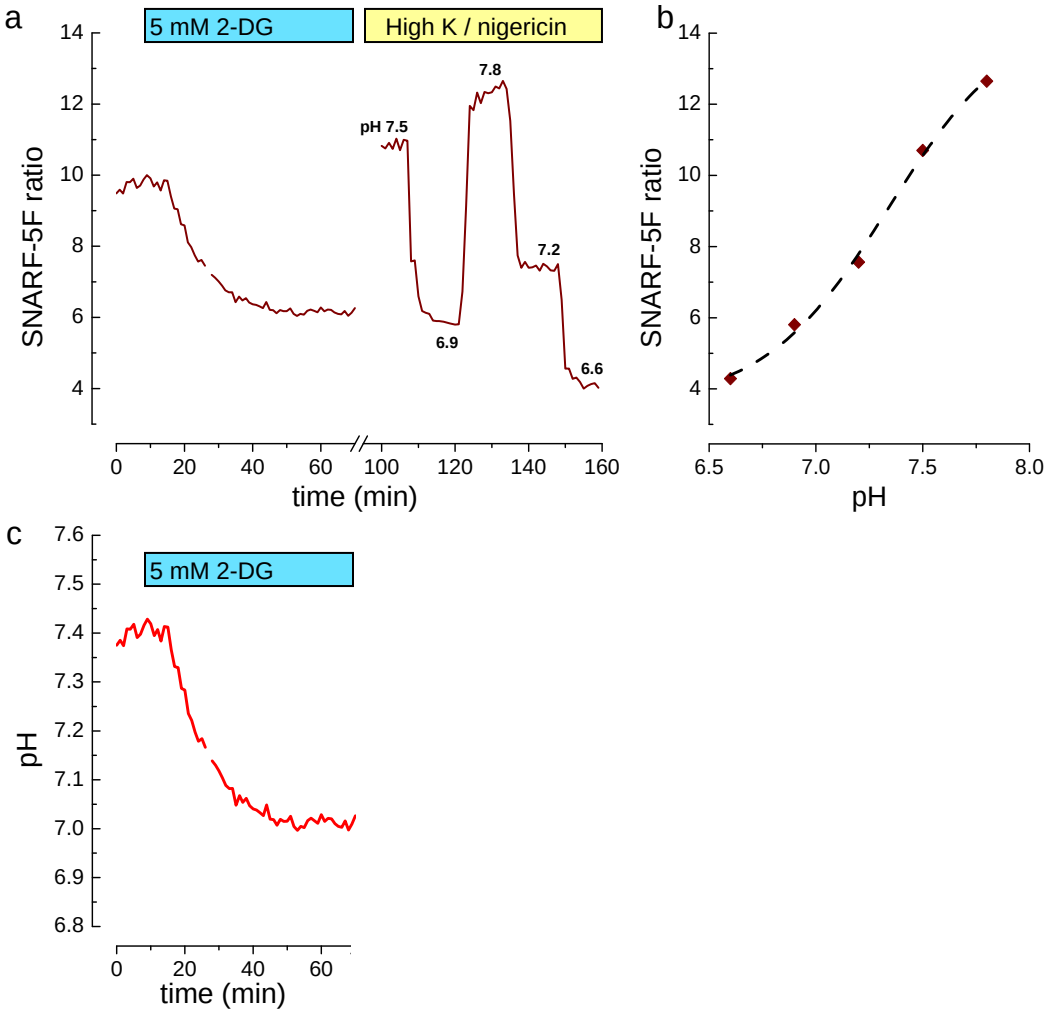

Supplementary Figure 7 | pH calibration using nigericin **(a)** Raw SNARF-5F signal for the experiment described in **Fig. 5a**. Application of 5 mM 2-DG leads to a decrease in SNARF-5F signal (indicating an intracellular acidification). Following a 30 minute incubation in a high potassium solution containing the ionophore nigericin (pH 7.5), the SNARF-5F signal is calibrated by washing in high K solutions of varying pH (in the constant presence of nigericin). **(b)** The standard SNARF-5F values are plotted against pH, and the data are fit with a sigmoid function which is used to calibrate the experimental SNARF-5F values to pH values in panel **(c)**.

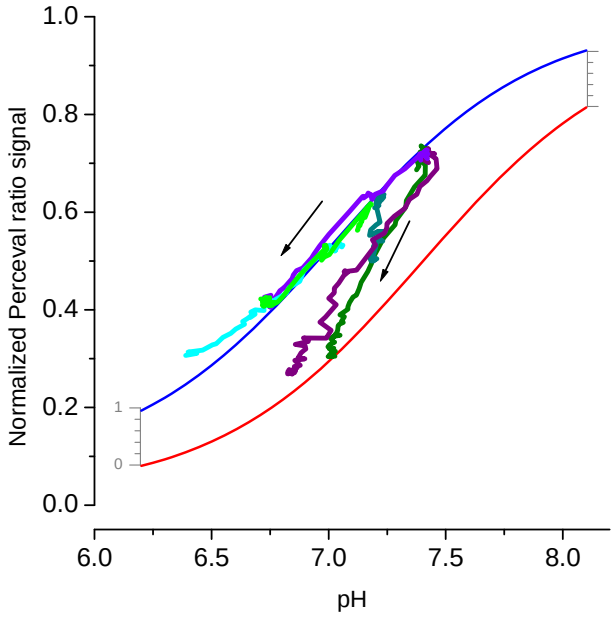

Supplementary Figure 8 | pH correction of 2DG and pH-control experiments As in Figure 5, experiments were performed either with wash-in of 5 mM 2-DG (dark green, blue and purple) or with exchange of extracellular solution to lower pH (light green, blue and purple). As in **Figure 5c**, the normalized Perceval signals from each experiment are plotted against calibrated pH values determined from concurrent SNARF-5F measurements.

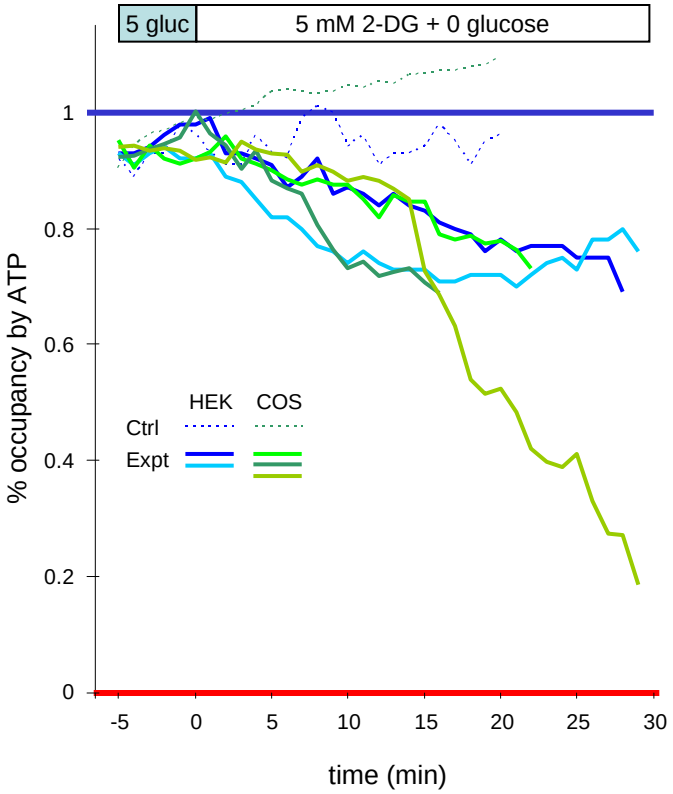

Supplementary Figure 9 | Comparable response of sensor in HEK293 and COS7 cells.

The pH-corrected Perceval occupancy is shown for control experiments in 5 mM glucose (dotted lines), and for experiments in which 2-deoxyglucose was substituted for glucose. Experiments on individual HEK293 cells are shown in blue colors and COS7 cells in green colors.

Supplementary Figure 10 | Perceval DNA and protein sequences.
The complete DNA coding sequence and protein sequence of Perceval.

```
+1     M  K  K  V  E  S  I  I  R  P  E  K  L  E  I  V  K  K  A  L
1   ATGAAAAAGG TGGAATCCAT CATCAGGCCC GAAAAGCTGG AGATCGTTAA GAAGGCTCTC
+1     S  D  A  G  Y  V  G  M  T  V  S  E  V  K  G  T  G  V  Q  G
61  TCGGACGCTG GATATGTGGG TATGACAGTC TCTGAGGTCA AGGGCACGGG CGTCCAGGGC
+1     G  I  V  E  R  Y  R  G  R  E  Y  S  A  G  Y  N  S  D  N  V
121 GGCATCGTCG AGAGGTACCG AGGAAGGGAG TACTCTGCAG GCTACAACAG CGACAACGTC
+1     Y  I  T  A  D  K  Q  K  N  G  I  K  A  N  F  K  I  R  H  N
181 TATATCACCG CCGACAAGCA GAAGAACGGC ATCAAGGCCA ACTTCAAGAT CCGCCACAAC
+1     I  E  D  G  G  V  Q  L  A  D  H  Y  Q  Q  N  T  P  I  G  D
241 ATCGAGGACG GCGGCGTGCA GCTCGCCGAC CACTACCAGC AGAACACCCC CATCGGCGAC
+1     G  P  V  L  L  P  D  N  H  Y  L  S  F  Q  S  K  L  S  K  D
301 GGCCCCGTGC TGCTGCCCGA CAACCACTAC CTGAGCTTCC AGTCCAAGCT GAGCAAAGAC
+1     P  N  E  K  R  D  H  M  V  L  L  E  F  V  T  A  A  G  I  T
361 CCCAACGAGA AGCGCGATCA CATGGTCCTG CTGGAGTTCG TGACCGCCGC CGGGATCACT
+1     L  G  M  D  E  L  Y  K  G  G  S  G  G  M  V  S  K  G  E  E
421 CTCGGCATGG ACGAGCTGTA CAAGGGCGGT TCCGGAGGCA TGGTGAGCAA GGGCGAGGAG
+1     L  F  T  G  V  V  P  I  L  V  E  L  D  G  D  V  N  G  H  K
481 CTGTTCACCG GGGTGGTGCC CATCCTGGTC GAGCTGGACG GCGACGTAAA CGGCCACAAG
+1     F  S  V  S  G  E  G  E  G  D  A  T  Y  G  K  L  T  L  K  L
541 TTCAGCGTGT CCGGCGAGGG CGAGGGCGAT GCCACCTACG GCAAGCTGAC CCTGAAGCTG
+1     I  C  T  T  G  K  L  P  V  P  W  P  T  L  V  T  T  L  G  Y
601 ATCTGCACCA CCGGCAAGCT GCCCGTGCCC TGGCCCACCC TCGTGACCAC CCTGGGCTAC
+1     G  L  Q  C  F  A  R  Y  P  D  H  M  K  Q  H  D  F  F  K  S
661 GGCCTGCAGT GCTTCGCCCG CTACCCCGAC CACATGAAGC AGCACGACTT CTTCAAGTCC
+1     A  M  P  E  G  Y  V  Q  E  R  T  I  F  F  K  D  D  G  N  Y
721 GCCATGCCCG AAGGCTACGT CCAGGAGCGC ACCATCTTCT TCAAGGACGA CGGCAACTAC
+1     K  T  R  A  E  V  K  F  E  G  D  T  L  V  N  R  I  E  L  K
781 AAGACCCGCG CCGAGGTGAA GTTCGAGGGC GACACCCTGG TGAACCGCAT CGAGCTGAAG
+1     G  I  D  F  K  E  D  G  N  I  L  G  H  K  L  E  Y  N  G  T
841 GGCATCGACT TCAAGGAGGA CGGCAACATC CTGGGGCACA AGCTGGAGTA CAACGGCACC
+1     I  V  D  L  I  P  K  V  K  I  E  L  V  V  K  E  E  D  V  D
901 ATAGTAGATC TGATCCCTAA GGTAAAAATT GAGCTCGTGG TGAAGGAGGA GGACGTCGAT
+1     N  V  I  D  I  I  C  E  N  A  R  T  G  N  P  G  D  G  K  I
961 AACGTGATAG ACATTATTTG CGAAAATGCC CGCACAGGTA ACCCCGGCGA CGGTAAGATA
+1     F  V  I  P  V  E  R  V  V  R  V  R  T  K  E  E  G  A  S  G
1021 TTTGTGATCC CAGTGGAGCG AGTGGTCAGG GTGCGAACCA AAGAGGAGGG AGCATCTGGT
+1     G  G  S  G  G  G  G  A  S  G  M  K  K  V  E  A  I  I  R  P
1081 GGTGGATCCG GTGGAGGAGG TGCGTCTGGT ATGAAAAAGG TGGAAGCTAT CATCAGACCC
+1     E  K  L  E  I  V  K  K  A  L  S  D  A  G  Y  V  G  M  T  V
1141 GAAAAGCTGG AGATCGTTAA AAAGGCTCTT TCCGACGCCG GATATGTGGG TATGACAGTC
+1     S  E  V  K  G  R  G  A  G  G  G  D  L  I  P  K  V  K  I  E
1201 TCTGAGGTCA AAGGCCGCGG TGCAGGTGGA GGGGATCTGA TCCCTAAGGT AAAAATTGAG
+1     L  V  V  K  E  E  D  V  D  N  V  I  D  I  I  C  E  N  A  R
1261 CTCGTGGTGA AGGAGGAGGA CGTCGATAAC GTGATAGACA TTATTTGCGA AAATGCCCGC
+1     T  G  N  P  G  D  G  K  I  F  V  I  P  V  E  R  V  V  R  V
1321 ACAGGTAACC CCGGCGACGG TAAGATATTT GTGATCCCAG TGGAGCGAGT GGTCAGGGTG
+1     R  T  K  E  E  G  A  S  G  G  G  G  G  S  G  G  A  S  G  M
1381 CGAACCAAAG AGGAGGGAGC ATCTGGTGGA GGTGGCGGTT CCGGAGGTGC ATCTGGTATG
+1     K  K  V  E  A  I  I  R  P  E  K  L  E  I  V  K  K  A  L  S
1441 AAAAAGGTGG AAGCTATCAT CAGACCCGAA AAGCTGGAGA TCGTTAAAAA GGCTCTTTCC
+1     D  A  G  Y  V  G  M  T  V  S  E  V  K  G  R  G  A  G  G  G
1501 GACGCCGGAT ATGTGGGTAT GACAGTCTCT GAGGTCAAAG GCCGCGGTGC AGGTGGAGGG
+1     D  L  I  P  K  V  K  I  E  L  V  V  K  E  E  D  V  D  N  V
1561 GATCTGATCC CTAAGGTAAA AATTGAGCTC GTGGTGAAGG AGGAGGACGT CGATAACGTG
+1     I  D  I  I  C  E  N  A  R  T  G  N  P  G  D  G  K  I  F  V
1621 ATAGACATTA TTTGCGAAAA TGCCCGCACA GGTAACCCCG GCGACGGTAA GATATTTGTG
+1     I  P  V  E  R  V  V  R  V  R  T  K  E  E  G  K  E  A  L
1681 ATCCCAGTGG AGCGAGTGGT CAGGGTGCGA ACCAAAGAGG AGGGAAAGGA AGCATTG
```

SUPPLEMENTARY RESULTS

A detailed explanation of the ratio-sensing behavior of the sensor

The GlnK1 – cpmVenus construct QV5 has two key properties: 1) It binds both ATP and ADP with extremely high affinity, with its affinity for ATP about 5-fold higher than that of ADP; and 2) ATP, but not ADP, binding produces a maximal fluorescence response. A general model to describe ATP and ADP binding to the sensor is

$$S{\cdot}ADP \underset{ADP}{\rightleftharpoons} S \overset{ATP}{\rightleftharpoons} S^*{\cdot}ATP$$

where S indicates the sensor, bound to either ADP or ATP (with the asterisk identifying the ATP-bound state as maximally fluorescent). Because of its high affinity, at physiologic nucleotide levels the population of sensor in the unoccupied state (S) is vanishingly small. With this approximation, we can calculate the relative occupancy of just the two remaining states: the occupancy of S·ADP is proportional to [ADP] / K_{ADP} and the occupancy of S*·ATP is proportional to [ATP] / K_{ATP}. The fraction of sensor in the ATP-bound (high fluorescence) state is then:

$$f_{ATP\text{-}bound} = \frac{\frac{[ATP]}{K_{ATP}}}{\frac{[ATP]}{K_{ATP}} + \frac{[ADP]}{K_{ADP}}}$$

Multiplying the numerator and the denominator by (K_{ATP}/[ADP]) gives the simplified equation:

$$f_{ATP\text{-}bound} = \frac{\overbrace{\frac{[ATP]}{[ADP]}}^{=R}}{\frac{[ATP]}{[ADP]} + \overbrace{\frac{K_{ATP}}{K_{ADP}}}^{=K_R}} = \frac{R}{R + K_R}$$

For simplicity, we have defined the ratio of nucleotide concentrations as R, and the ratio of the affinity of the probe for ATP and ADP as K_R. We expect K_R to be an intrinsic feature of the sensor, so the fluorescent response is determined by the R, or ratio of ATP to ADP. The dependence takes the form of a familiar binding equation, where K_R is the value of the [ATP] / [ADP] ratio that produces a half-

maximal fluorescence response. The QV5 construct is five-fold more sensitive to ATP than ADP, so we predict $K_R \approx 0.2$. This corresponds well to the actual behavior (**Figure 2** in the main paper).

pH and chloride sensitivity of the ATP sensor

We found that, as for the other probes based on circularly permuted fluorescent proteins[1, 2], the fluorescence intensity of the QV5 construct was sensitive to changes in pH. Cuvette experiments on purified QV5 construct showed that when excited at 490 nm, the fluorescence intensity for each form of the sensor (nucleotide free, ADP-bound, half maximal ATP, and full ATP) had greatest intensity at alkaline pH, and then diminished as the solution was acidified (**Supplementary Figure 1**). This translates to a 490 nm / 405 nm ratio signal that also is highest at alkaline pH values. The fluorescence with 435 nm excitation also diminished with acidification, but at all pH's measured this signal was invariant with ATP/ADP occupancy (although there was some change in fluorescence when the binding site was vacant, in the absence of any nucleotide).

The fact that alkaline pH leads to increased fluorescence is seen for most GFP-based fluorescent proteins, as protonation of the fluorescent protein's chromophore leads to a quenching of the fluorescence[3, 4]. With the QV5 construct, although the absolute intensity of the fluorescence is altered by pH, the response to ATP is relatively insensitive to changes in pH. This is evident from the fact that the curves for the different states of the sensor (**Supplementary Fig. 1b,c**) are approximately parallel in the range of cellular pH, indicating that the response to ATP does not change significantly across varying pH values. This does not indicate that pH should be of no concern (the fluorescence and ratio are still very much pH sensitive); it does mean, however, that changes in ATP/ADP can still be measured, even at different pH levels. Additionally, if the changes in pH are identified, then the sensor signal can be corrected for such changes.

We next assayed for any effect that changes in chloride might have on the responsiveness of the QV5 construct, as other FP's can exhibit chloride sensitivity[5]. We found that although a change in chloride concentration from 0 to 100 mM quenched the overall fluorescence signal of the QV5 construct by about 20% (**Supplementary Fig. 1d**), the ratio and responsiveness to ATP remained unchanged.

Correcting for changes in intracellular pH

Glycolytic inhibition can lead to a change in intracellular pH as well as energy charge (see the pH change in **Fig. 5a** of the main paper). By measuring the pH simultaneously with the Perceval signal

(using the pH indicator SNARF-5F), we were able to use the known pH dependence from the cuvette measurements to isolate the ATP/ADP signal from any pH-induced changes in fluorescence.

To correct the Perceval signal for pH, the Perceval signal was plotted against pH (**Fig. 5** and **Supplementary Fig. 8**). The pH sensitivity curves of the ATP-bound and ADP-bound sensor from the cuvette experiments were scaled using a single factor and we made the assumption that the sensor is near the fully ATP bound state at the beginning (fully-fed portion) of an experiment (in this case we assumed ATP/ADP = ~4, which corresponds to an occupancy of ~0.93). For each point in time, the Perceval signal can then be adjusted to where it falls between the maximum [ATP-bound] curve (set to a value of 1) and the minimum [ADP-bound] curve (set to 0).

To validate this method of pH correction, we also performed a pure pH challenge to HEK cells expressing Perceval and loaded with SNARF-5F. By lowering the extracellular pH, we were able to induce an intracellular acidification similar in magnitude to the pH change seen during metabolic inhibition. When the Perceval signal was pH-corrected, it remained around the maximally activated state (1.0) for the duration of the challenge.

Sensitivity of the GlnK1 – cpmVenus construct to Mg^{2+} ions

One of the primary differences in the crystal structure of the GlnK1 protein bound to ADP compared to that bound to ATP is the fact that the ATP is complexed with a Mg^{2+} ion whereas the ADP is not[6]. We therefore determined the effect of [Mg^{2+}] on the properties of the GlnK1 – cpmVenus QV5 construct (**Supplementary Figure 2**).

ATP We first determined whether magnesium is required for the full agonist effect of ATP. Addition of sodium ATP and chelation of any contaminating magnesium by addition of EDTA leads to the same submaximal fluorescence response seen with ADP (**Supplementary Fig. 2,** *green squares*). This leads us to conclude that free ATP likely acts as an incomplete agonist, in a similar manner to ADP. Subsequent addition of magnesium to the ATP solution led to a maximal response, so we conclude that the full fluorescence response is due to MgATP binding. These results are compatible with the conclusion of Yildiz et al.[6] that the Mg^{2+} ion bound together with ATP is essential for stabilizing the closed state of the T-loop.

ADP The affinity of ADP for Mg^{2+} is much weaker than that of ATP, and it seemed possible that the sensor might be simply a Mg^{2+} sensor whose affinity depended on which nucleotide was bound. To investigate the possibility that a maximal fluorescence effect could be produced by Mg^{2+} in the binding site – regardless of whether ATP or ADP is bound -- we added potassium ADP to the sensor in the absence of any free Mg^{2+}. This gave a response identical to the MgADP response seen in control experiments. To investigate the effect of Mg^{2+} on the ADP-bound sensor, we then added $MgCl_2$ to the solution (**Supplementary Fig. 2**, *red circles*). If Mg^{2+} bound to the ADP-bound sensor could produce a maximal response, then we would expect a curve with a response similar to what we saw with the Mg^{2+} addition to ATP (but with higher Mg^{2+} concentrations required due to the lower Mg^{2+} affinity of ADP). We observed the opposite result: upon $MgCl_2$ addition, there was a slight decrease in the fluorescent signal. We conclude that Mg^{2+} plus ADP does not produce the same maximal response as MgATP.

Finally, we investigated whether MgADP competes with free ADP, free ATP and MgATP for GlnK1 binding. To do this, we took advantage of the different relative affinities of ATP and ADP for Mg^{2+}. By adding $MgCl_2$ to a mixture of ATP and ADP, we were able to predict significantly different outcomes for whether MgADP is competing for the site or not. In each case, as we add $MgCl_2$ we should see a fast increase in fluorescence as Mg^{2+} binds to the high affinity ATP and produces a response proportional to the ATP / ADP ratio. If MgADP binds in the pocket and acts identically to free ADP, then we should see no further effect on the fluorescence as Mg^{2+} binds to ADP (at higher concentrations of $MgCl_2$ due to its lower affinity). If, however, MgADP does not bind to the site, as we increase the $[Mg^{2+}]$, we should see an increase in the signal as the free [ADP] is lowered by the Mg^{2+}. This second scenario is what the data show (**Supplementary Fig. 2,** *blue diamonds*): as Mg^{2+} was added to the solution, the response appeared more and more like ATP alone rather than as a mixture of ATP and ADP.

In summary, it appears that only MgATP is capable of producing the conformational change that leads to the maximal fluorescence change in our sensor. The non-Mg^{2+}-bound ATP and ADP species compete with MgATP and produce only a small change in fluorescence, while MgADP does not change fluorescence or compete for binding sites.

SUPPLEMENTARY METHODS

Random library construction. A pair of long oligonucleotides with complementary 3' ends was used to synthesize the N-terminal (pre-*Kpn*I site) or C-terminal (post-*Bgl*II site) coding sequence of GlnK1. Selected sites in each oligonucleotide were synthesized using a doped mixture of nucleotides, corresponding to 97% of the wild-type nucleotide and 1% each of the other nucleotides. For each section of the coding sequence, the two oligonucleotides (each one constituting a pool of mutant sequences) were combined, annealed, and subjected to a single primer extension reaction with Taq polymerase. The full-length product was cut with appropriate restriction enzymes and ligated into a previously prepared sensor construct. Each individual transformant colony was streaked onto a sector of a selective bacterial plate and allowed to grow before screening. Two libraries were prepared, one with mutations in the N-terminal half and the other with mutations in the C-terminal half. Each library pool had approximately 30 base sites with potential mutations, so that the average nominal mutation rate was approximately one mutation per colony.

Materials. Oligonucleotides were purchased from Integrated DNA Technologies (Coralville, IA), and custom gene synthesis was performed by Genscript (Piscataway, NJ; web:www.genscript.com).

Protein expression and purification. Cuvette experiments: To eliminate coassembly with native GlnK and GlnB subunits, his_7-tagged proteins were expressed in the *ΔglnB*, *ΔglnK* strain UNF3435 (ref. 8) generously provided by Mike Merrick, John Innes Centre, Norwich, UK. Bacteria were grown in aerated liquid culture for 24 hours at 37°C, and then transferred to room temperature for an additional 24 hours. Bacteria were then centrifuged and lysed with the CelLytic B reagent (Sigma). Proteins were purified using a Ni-NTA Spin Kit (QIAGEN, Valencia, CA) according to manufacturer's instructions. 96 well plate experiments: Individual colonies of bacteria were picked and streaked onto sectors of agar plates. Following 24 hours at 37°C, plates were transferred to 4°C, and incubated for 4 to 7 days to allow protein expression. Bacteria were then transferred from the sector of the agar plate to a well in a 96 well plate and resuspended in 2xYT media. The bacteria were then transferred to a 96 well iLAP plate (H9412 from Sigma, St. Louis, MO) for lysis and Ni^{2+} chelate binding and were incubated at 4°C overnight. The wells were then washed according to manufacturer's instructions and the proteins were eluted with the standard MOPS buffer (see recipe below), with the addition of 20 mM imidazole and 0.1% bovine serum albumin (BSA), pH 7.3 for 1 hour at room temperature. The proteins were then transferred to a 96 well plate (Corning Costar, Lowell, MA) that had been blocked with the BSA solution overnight.

Fluorometry. Cuvette Experiments: Aliquots of purified sensor protein were added to a cuvette containing 100 mM MOPS, 50 mM KCl, 5 mM NaCl, and 0.5 mM $MgCl_2$, pH 7.3 with KOH, unless otherwise noted. All nucleotides were added with Mg^{2+} concentration calculated to remain at 0.5 mM free Mg^{2+} (buffer calculations were based on the stability constants from ref. 9 and confirmed in several cases by fluorescence measurements with mag-fura-2). Fluorescence was measured using a Fluorolog-3, HORIBA Jobin Yvon (Edison, NJ). For all excitation experiments, slit widths were set at 2 nm for excitation wavelength and 10 nm for emission wavelength. For excitation spectra, the excitation range was 380 nm to 510 nm, with readings taken every 2 nm. Emission wavelength was 530 nm (slit width 5 nm) with an integration time of 1 s. For all other excitation data, measurements were taken at 405, 435, and 495 nm, with emission read at 520 nm. For each point, 3 scans, each with a 0.3 s integration time, were averaged. For kinetic determination, the excitation wavelength was 500 nm, emission at 525 nm, integration time 0.3 s, samples taken with a 1 s interval.

Cellular imaging. Human embryonic kidney 293 cells (HEK293) and COS-7 (American Type Culture Collection, Manassas, VA) were transiently transfected with a Perceval expression plasmid using electroporation. For experiments using SNARF-5F, 10 μM of the acetomethoxy ester form of the dye (Invitrogen, Carlsbad, CA) was loaded into the cells for 30 minutes prior to imaging in a dye-free solution. During imaging, the solution supply was constantly bubbled with 95% air and 5% CO_2 (calculated to give a pH of 7.3) and delivered through a flow-through heater (Warner Instruments, Hamden, CT) at a temperature of 31–33°C. Unless otherwise specified, the extracellular solution was composed of (in mM): 129.5 NaCl, 25 $NaHCO_3$, 10 D-glucose, 2.5 KCl, 1.25 NaH_2PO_4, 2 $CaCl_2$, and 1 $MgCl_2$. In experiments with 2-deoxyglucose, 5 mM 2-deoxyglucose was substituted for 10 mM glucose.

Imaging was performed with a pco (Kelheim, Germany) Sensicam QE CCD camera mounted on an Olympus Optical (Tokyo, Japan) BX51 upright microscope equipped with a 60x, 0.9 numerical aperture (NA) objective. A rapid wavelength switching monochromator (Polychrome IV; T.I.L.L. Photonics, Gräfelfing, Germany) with a 12.5 nm slit width was used for fluorescence excitation in conjunction with a 515 nm dichroic mirror (515DCXR) and a 535/25 nm band pass filter (D535/25) for collecting Perceval fluorescence emission. The SNARF-5F signal was obtained by exciting at 540 nm and alternating between a cube containing a Q565LP dichroic mirror + D585/20 nm band pass filter and Q595LP dichroic mirror + HQ645/75 nm band pass filter. The ratio of these two emission wavelengths

reports the intracellular pH. All filters were purchased from Chroma Technology (Rockingham, VT). Backgrounds were subtracted from each image by taking the average of a cell-free region of the image and subtracting that value from each image prior to analysis.

pH control and calibration

For experiments where extracellular pH was modified, $NaHCO_3$ was lowered to 10 mM [pH 6.9] or 5 mM [pH 6.6] (sodium balanced with NaCl). For experiments in which SNARF-5F was used to determine intracellular pH, the SNARF-5F signal was calibrated by using the high K^+/nigericin method[7]; for an example of this calibration method, see **Supplementary Figure 7**. Calibration solution contained 5 µg/ml nigericin in a high [K^+] bathing solution: (in mM) 130 KCl, 10 NaCl, 2 $CaCl_2$, 1 $MgCl_2$, 10 MOPS, pH 7.8 with KOH. Additional pH solutions (pH 7.5, 7.2, 6.9 and 6.6) were made by adding MOPS in the acid form to the pH 7.8 solution.

REFERENCES

1. Nagai, T., Sawano, A., Park, E. S., & Miyawaki, A. Circularly permuted green fluorescent proteins engineered to sense Ca2+. *Proc Natl Acad Sci U S A* **98**, 3197–3202 (2001).
2. Belousov, V. V., Fradkov, A. F., Lukyanov, K. A., Staroverov, D. B., Shakhbazov, K. S., Terskikh, A. V., & Lukyanov, S. Genetically encoded fluorescent indicator for intracellular hydrogen peroxide. *Nat Methods* **3**, 281–286 (2006).
3. Brejc, K., Sixma, T. K., Kitts, P. A., Kain, S. R., Tsien, R. Y., Ormö, M., & Remington, S. J. Structural basis for dual excitation and photoisomerization of the Aequorea victoria green fluorescent protein. *Proc Natl Acad Sci U S A* **94**, 2306–2311 (1997).
4. Kneen, M., Farinas, J., Li, Y., & Verkman, A. S. Green fluorescent protein as a noninvasive intracellular pH indicator. *Biophys J* **74**, 1591–1599 (1998).
5. Nagai, T., Ibata, K., Park, E. S., Kubota, M., Mikoshiba, K., & Miyawaki, A. A variant of yellow fluorescent protein with fast and efficient maturation for cell-biological applications. *Nat Biotechnol* **20**, 87–90 (2002).
6. Yildiz, O., Kalthoff, C., Raunser, S., & Kühlbrandt, W. Structure of GlnK1 with bound effectors indicates regulatory mechanism for ammonia uptake. *EMBO J* **26**, 589–599 (2007).
7. Thomas, J. A., Buchsbaum, R. N., Zimniak, A., & Racker, E. Intracellular pH measurements in Ehrlich ascites tumor cells utilizing spectroscopic probes generated in situ. *Biochemistry* **18**, 2210–2218 (1979).

8. Arcondeguy, T., van Heeswijk, W.C, & Merrick, M. Studies on the roles of GlnK and GlnB in regulating *Klebsiella pneumoniae* NifL-dependent nitrogen control. *FEMS Microbiology Lett.* **180**, 263-270 (1999).
9. Martell, A.E., & Smith, R.M. NIST Standard Reference Database 46 Version 8.0; NIST critically selected stability constants of metal complexes. National Institute of Standards and Technology (2004).